JOURNAL OF ENVIRONMENTAL SCIENCES 119 (2022) 78–92

Available online at www.sciencedirect.com

ScienceDirect

www.elsevier.com/locate/jes

JES JOURNAL OF ENVIRONMENTAL SCIENCES

www.jesc.ac.cn

Understanding the risks of mercury sulfide nanoparticles in the environment: Formation, presence, and environmental behaviors

Pei Lei[1,**], *Nan Zou*[1,**], *Yujiao Liu*[1], *Weiping Cai*[2,3], *Mengjie Wu*[1], *Wenli Tang*[1], *Huan Zhong*[1,4,*]

[1] *State Key Laboratory of Pollution Control and Resource Reuse, School of Environment, Nanjing University, Nanjing 210023, China*

[2] *Key Laboratory of Soil Environment and Pollution Remediation, Institute of Soil Science, Chinese Academy of Sciences, Nanjing 210008, China*

[3] *University of Chinese Academy of Sciences, Beijing 100049, China*

[4] *Environmental and Life Sciences Program (EnLS), Trent University, Peterborough Ontario, K9L 0G2, Canada*

ARTICLE INFO

Article history:
Received 24 October 2021
Revised 16 January 2022
Accepted 10 February 2022
Available online 26 February 2022

Keywords:
Bioavailability
Bioaccumulation
Organic matter
Mercury methylation
Dissolution
Aggregation

ABSTRACT

Mercury (Hg) could be microbially methylated to the bioaccumulative neurotoxin methylmercury (MeHg), raising health concerns. Understanding the methylation of various Hg species is thus critical in predicting the MeHg risk. Among the known Hg species, mercury sulfide (HgS) is the largest Hg reservoir in the lithosphere and has long been considered to be highly inert. However, with advances in the analytical methods of nanoparticles, HgS nanoparticles (HgS NPs) have recently been detected in various environmental matrices or organisms. Furthermore, pioneering laboratory studies have reported the high bioavailability of HgS NPs. The formation, presence, and transformation (e.g., methylation) of HgS NPs are intricately related to several environmental factors, especially dissolved organic matter (DOM). The complexity of the behavior of HgS NPs and the heterogeneity of DOM prevent us from comprehensively understanding and predicting the risk of HgS NPs. To reveal the role of HgS NPs in Hg biogeochemical cycling, research needs should focus on the following aspects: the formation pathways, the presence, and the environmental behaviors of HgS NPs impacted by the dominant influential factor of DOM. We thus summarized the latest progress in these aspects and proposed future research priorities, e.g., developing the detection techniques of HgS NPs and probing HgS NPs in various matrices, further exploring the interactions between DOM and HgS NPs. Besides, as most of the previous studies were conducted in laboratories, our current knowledge should be further refreshed through field observations, which would help to gain better insights into predicting the Hg risks in natural environment.

* Corresponding author.
E-mail: zhonghuan@nju.edu.cn (H. Zhong).
** These authors contributed equally to this work.

https://doi.org/10.1016/j.jes.2022.02.017
1001-0742/

Introduction

Mercury (Hg) is a natural and ubiquitous trace metal, but is considered a priority contaminant, particularly its organic form methylmercury (MeHg), causing risks to wildlife and human health (Bravo and Cosio, 2020; Haskins et al., 2020; Rodrigues et al., 2019). Being highly bioavailable, MeHg could biomagnify in food webs, elevating its concentrations to be millions of fold higher in food (e.g., up to 3300 μg/kg in fish (Lino et al., 2019)) than that in the environment, and impairing cognitive ability of humans via dietary exposure (Sunderland and Selin, 2013). For instance, it was estimated that MeHg exposure in Europe leads to an intelligence quotient (IQ) reduction of 1.5-2 million newborns per year (Sunderland and Selin, 2013); while in China, dietary exposure of MeHg incurs an average decrease in newborn IQ of 0.14 (Chen et al., 2019). Therefore, a comprehensive understanding of the methylation of various Hg species, principally mediated by diverse microorganisms, is critical in predicting the Hg risks to both wildlife and human beings (Lei et al., 2021b).

Microbial Hg methylation is determined by both microbial activity and Hg bioavailability in the environment (Lei et al., 2021a; Regnell and Watras, 2019), of which the bioavailability of inorganic Hg is determined by its chemical speciation (Hsu-Kim et al., 2013). Among the known Hg species, HgS is the most abundant in the lithosphere (Smith et al., 2015). HgS has long been recognized as the most insoluble Hg species due to the low solubility (pK_{sp} = 55.9-50.9) (Benoit et al., 1999; Drott et al., 2013; Jiang et al., 2016) and could hardly be microbially transformed (Clever et al., 1985; Dong et al., 2016). The formation and then precipitation of HgS particles could effectively remove Hg from further environmental cycles (Barnett et al., 1997; Smith et al., 2015; Wolfenden et al., 2005). However, recent studies revealed that nano-scaled HgS (referred to as HgS NPs), in contrast to its larger counterpart, is chemically active and bioavailable to methylation microbes (Hsu-Kim et al., 2013). The high bioavailability of HgS NPs was verified in a few pioneering studies, reporting that HgS NPs could be methylated by microorganisms in laboratory tests. For instance, *Desulfovibrio desulfuricans* ND132 (a typical strain of sulfate-reducing bacteria, SRB) could methylate 6%-10% of spiked HgS NPs (with a mean diameter of 3-4 nm) into MeHg (Zhang et al., 2014). Similar results have also been obtained when incubating HgS NP-spiked sediments in the laboratory (Aiken et al., 2011; Ly et al., 2021; Mazrui et al., 2016; Pham et al., 2014; Yu et al., 2018). Similar to other metallic nanoparticles such as $Au^{(0)}$ NPs, $Ag^{(0)}$ NPs, TiO_2 NPs, CeO_2 NPs, CuO NPs, and ZnO NPs (Philippe and Schaumann, 2014; Wang et al., 2016), dissolved organic matter (DOM) is found to be an important factor that impacts the transformation and fate of HgS NPs in the environment (Mazrui et al., 2018). The relationship between DOM characteristics (e.g., molecular weight, aromaticity, and specific components) and HgS NP bioavailability have been revealed in a couple of studies (Graham et al., 2012; Poulin et al., 2017), while all of which were conducted under laboratory conditions. Natural DOM is highly heterogeneous, making it difficult to understand the complex interactions between HgS NPs and DOM. Those recent studies suggested the possibility of microbial methylation of HgS NPs, highlighting the necessity of rethinking the role of HgS in Hg biogeochemical cycles.

The potential risks of HgS NPs to organisms depends on both their concentrations and bioavailability in the environment. In recent years, some studies have shown the occurrence of HgS NPs in different environmental matrices (e.g., soils, minerals), organisms (e.g., plants), traditional medicines, and even human body fluids (Barnett et al., 1997; Janadri et al., 2015; Lowry et al., 2004; Lu et al., 2020; Patty et al., 2009; Yan, 2007). However, the concentrations and bioavailability of HgS NPs, as well as the dominant factors affecting the bioavailability of HgS NPs in various environmental matrices/organisms are still unclear, making it questionable whether HgS NPs are an important pool of bioavailable Hg in the biosphere. To address these issues, we summarize recent progress in the formation of HgS NPs via abiotic and biotic pathways, the presence of HgS NPs in various environmental matrices and organisms, as well as the methylation of HgS NPs mediated by DOM. We then suggest future avenues in understanding the risks of HgS NPs in the environment. The knowledge summarized in this review would help rethink the role of HgS NPs in the biogeochemical cycling of Hg and provide the wisdom of protecting organisms from Hg bioaccumulation.

1. The formation of HgS NPs

Understanding the formation of HgS NPs would help to predict their presence in the environment and organisms. In the environment, HgS NPs could be generated by either abiotic or biotic processes with Hg^{2+} as the Hg precursor, which depends on whether organisms are directly involved (Chen et al., 2017). For clarity, when the systems do not involve organisms directly, the formation of HgS NPs was recognized as an abiotic process; when the systems directly involve organisms, the formation is classified as biological pathways. The abiotic formation of HgS NPs could occur in the Hg^{2+}-DOM binary system, Hg^{2+}-DOM-S^{2-} ternary system, and Hg^{2+}-FeS system, while the biotic formation could be driven by microorganism-mediated and other biologically-mediated generation processes (Fig. 1).

1.1. *Abiotic formation of HgS NPs*

In natural environment with low Hg^{2+}/DOM ratios (e.g., <1 μg Hg/mg DOM), Hg^{2+} in Hg^{2+}-DOM binary system preferentially combines with reduced sulfur sites on the DOM to form HgS and HgS NPs (Haitzer et al., 2002; Hesterberg et al., 2001) (Fig. 1A). It has been proven that sulfur-containing DOM (e.g., thiolate) directly leads to the formation of HgS NPs (3-5 nm) under aerobic conditions (Manceau et al., 2015), and the reaction mechanism was revealed by the molecular orbital calculations (Enescu et al., 2016). In the case of thiolate as a reducing sulfur source, the four-coordinated β-HgS can be obtained through the S-C bonds of the thiol group in $Hg(SR)_2$ continuously cleave and release alkyl groups, which would be transferred to another thiol and form a thioether. This dealkylation reaction is thermodynamically favorable, and the calculation result provides a strong theoretical basis for the abiotic

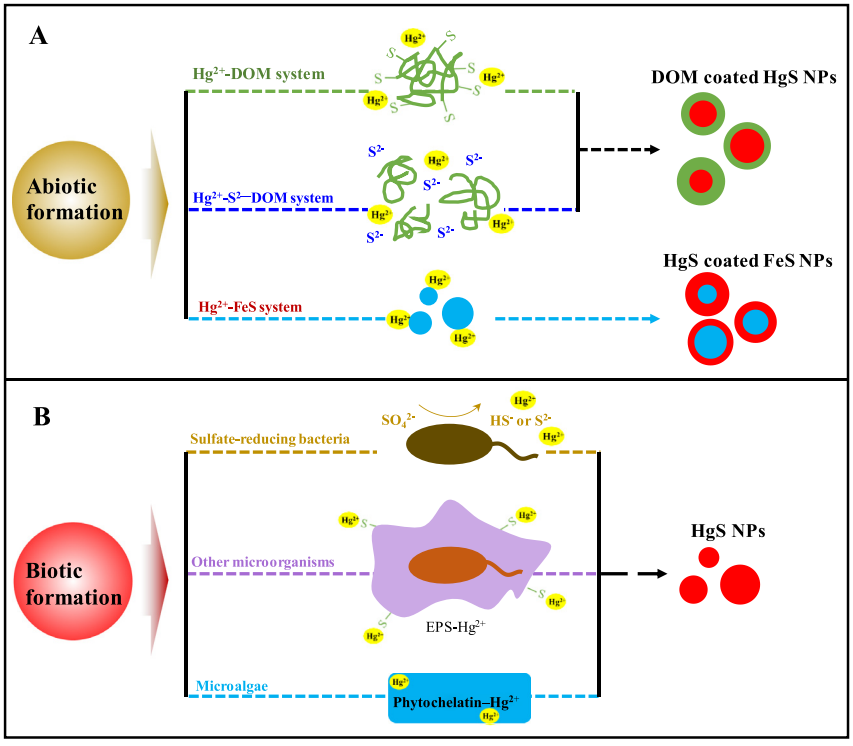

Fig. 1 – The abiotic (A) and biotic (B) formation of HgS NPs in the laboratory systems or natural environment. The abiotic formation of HgS NPs could occur in Hg^{2+}–dissolved organic matter (DOM) binary system, Hg^{2+}–DOM–S^{2-} ternary system, and Hg^{2+}–FeS system. Some microbial transformations, including sulfate reduction, secretion of extracellular polymer substances (EPS) by other microorganisms, and the production of phytochelatin by microalgae, are involved in the biotic formation of HgS NPs. This figure was modified from a previous report (Chen et al., 2017).

formation of HgS NPs under aerobic and catalyst-free conditions (Enescu et al., 2016).

The generation of HgS NPs in the Hg^{2+}-DOM binary system could be accelerated by light (Chen et al., 2017), which was presumably due to the direct photolysis of Hg-DOM or Hg-cysteine complexes that leads to the breakage of R–S bonds and formation of HgS solids or nanoparticles (Luo et al., 2017). Under UV irradiation (300–400 nm), thioglycolic acid solution (a model ligand) could transform $Hg(OOCCH_2S)$ into Hg^0 and spherical and rod-shaped HgS NPs (56–106 nm) (Si and Ariya, 2015). In photo-irradiated Hg^{2+}-DOM solution at a higher concentration of Hg^{2+} (0.1 mmol/L), $HgCl_2$ could also be transformed into HgS NPs with a diameter of ~500 nm (Luo et al., 2017).

In the Hg^{2+}-S^{2-}-DOM ternary system, the newly spiked Hg^{2+} would be rapidly captured by DOM to form Hg^{2+}-DOM complexes, which would diffuse into the hypoxic environment and react with abundant S^{2-} to further induce the formation of HgS NPs (Slowey, 2010) (Fig. 1A). DOM may play multiple roles in this system. On the one hand, some functional groups (e.g., thiols) in DOM have a strong affinity for Hg. Subsequently, the competition between these thiols and S^{2-} for Hg^{2+} may inhibit the formation of HgS NPs (Gerbig et al., 2011; Pham et al., 2014; Poulin et al., 2017). On the other hand, DOM may also act as the capping agent for newly formed HgS NPs to inhibit the aggregation of nanoparticles (Ravichandran et al., 1999). The properties and compositions of DOM, as well as the Hg/DOM concentration ratios, have been documented to impact the formation and transformation of HgS NPs (Chen et al., 2017).

Mackinawite (FeS) and pyrite (FeS_2) commonly exist in anaerobic sediments, and they can affect the geochemical cycle of heavy metals due to their high adsorption capacity (Morse and Luther, 1999; Murphy and Strongin, 2009). FeS could immobilize Hg^{2+} through precipitation and adsorption. Specifically, Hg^{2+} can adsorb onto the FeS surface and then gradually be transformed into HgS (Liu et al., 2008). Jeong et al., (2007, 2010) used X-ray diffraction (XRD) and scanning electron microscope (SEM) to further confirm HgS as the conversion product of Hg^{2+} immobilized by FeS. Moreover, co-precipitation of FeS and Hg^{2+} would lead to the precipitation of Hg-S-Fe nanoparticles (Jonsson et al., 2012). It has been observed that Hg-S-Fe composite nanoparticles (~30 nm) could be formed in the sediment pore water with transmission electron microscopy coupled with energy-dispersive X-ray spectroscopy (TEM-EDX) (Ji et al., 2020). The Hg-S-Fe nanoparticles may also have high bioavailability. Further studies should concentrate on the production conditions, structural characteristics, and bioavailability of HgS NPs in the Hg^{2+}-FeS system.

Similarly, thiols can readily form strong complexes with Hg^{2+} and partially inhibit the formation of HgS NPs and Hg-S-Fe NPs (Skyllberg and Drott, 2010). Some DOM could also maintain nanoparticle stability through absorbing to HgS NP surface. The impacts of DOM on the formation and aggregation

of HgS NPs depend on their composition and characteristics. It is necessary to pay more attention to the analysis of DOM to better understand their roles in the formation of HgS NPs in the Hg^{2+}-FeS system.

1.2. *Biotic formation of HgS NPs*

The biotic formation of HgS NPs is primarily driven by microorganisms (Fig. 1B). It is well known that the reducing sulfur (S^{2-}or HS^-) produced by anaerobic microorganisms can precipitate Hg^{2+} as HgS NPs (Aiking et al., 1985; Gilmour et al., 2011; Sathyavathi et al., 2013). Presumably, extracellular polymeric substances (EPS) produced by *Yarrowia* spp. could precipitate Hg^{2+} as HgS NPs through the sulfhydryl groups of protein molecules (Oyetibo et al., 2016). For example, Zhang et al. (2020) proposed that EPS produced by *D. desulfuricans* ND132 contained abundant sulfides, which can provide supersaturation conditions for the precipitation of HgS NPs.

In addition, single crystal HgS NPs (5-15 nm) and polycrystalline HgS NPs (10–200 nm) have also been observed in the cell wall of aquatic moss plants (Satake et al., 1990), although the sources of these HgS NPs are unknown (Fig. 1B). Some marine microalgae, e.g., green alga *Chlorella autotrophica*, flagellate *Isochrysis galbana*, and diatom *Thalassiosira weissflogii*, also have been proven to drive the conversion of Hg^{2+} to HgS NPs (Wu and Wang, 2014), and the intermediate of HgS NPs may be the Hg^{2+}-plant chelating protein complex (Kelly et al., 2007). Besides, Oyetibo et al. (2019) found the transformation of Hg^0 into HgS NPs by Hg-resistant yeasts *Yarrowia Idd1* & *Idd2* and the presence of HgS NPs in the EPS of the yeasts. It should be noted that Hg concentrations used in these experiments (generally in mM concentration) were much higher than the environmental concentrations (at the level of pM) due to the difficulty in characterizing HgS NPs at trace levels (Oyetibo et al., 2019; Patty et al., 2009; Wu and Wang, 2014). These further emphasize the necessity for developing more sensitive methods for detecting HgS NPs.

2. Presence of HgS NPs in nature

2.1. *Analytical methods of HgS NPs*

Due to the low concentration, inhomogeneity, and heteroaggregation of HgS NPs and background interferences, it is not straightforward to characterize and quantify HgS NPs in complex environmental and biological matrices (e.g., soil, sediment, plant, and mammal) (Cai et al., 2022; Chen et al., 2017). Nevertheless, a variety of analytical techniques (including electron microscopy, spectroscopy, energy spectroscopy, and mass spectrometry), have been developed and used for the qualitative and quantitative analysis of HgS NPs. The advantages and disadvantages of these methods were summarized as follows and the details are shown in Table 1.

A variety of nano-characterization techniques have been used in qualitative analysis of the compositions and sizes of HgS NPs. SEM and TEM could provide the morphologic and size information of HgS NPs. Equipped with energy-dispersive X-ray spectroscopy (EDX) and selected area electron diffraction (SAED), SEM/TEM could also give the elemental identification and crystallographic properties of nanoparticles (Scofield et al., 2015; Zhang et al., 2020). The presence of HgS NPs has been observed in soils (Barnett et al., 1997; Higueras et al., 2003), suspended matter (Kocman et al., 2011), and the cell wall of aquatic bryophytes (Satake et al., 1990) with the help of SEM/TEM.

Dynamic light scattering (DLS), as well as time-resolved DLS, could offer information about the hydrodynamic particle size of HgS NPs and help to observe the aggregation process of HgS NPs (Deonarine and Hsu-Kim, 2009). Combined with TEM, DLS showed that HgS NPs in the Hg-S-DOM mixture system would aggregate during the aging process, leading to a reduction in Hg bioavailability (Pham et al., 2014). It should be noted that this technique requires a high concentration of target particles (>1 Hg mg/L). Besides, DLS is susceptible to interference from environmental colloids (Deonarine and Hsu-Kim, 2009; Slowey, 2010), which could be attributed to the calculation of hydrodynamic size from this technique only depending on the motion of particles in the solution and ignoring the influences of inter-particle interaction (Pham et al., 2014).

X-ray absorption fine structure (XAFS), including X-ray absorption near-edge structure (XANES) and extended X-ray absorption fine structure (EXAFS), is a non-destructive analytical technique and requires no extraction, which has been widely used to characterize the Hg species as well as their structure and bonding in samples (Chen et al., 2017). With the help of EXAFS, it has been proved that DOM could limit HgS NP size to nanoscale as well as increase their disorder degree, illuminating the role of DOM plays in HgS NP formation and stabilization (Gerbig et al., 2011; Slowey, 2010). XAFS requires a high concentration of Hg, usually >100 mg/kg, which limits the application of XAFS in samples with a low concentration of Hg (Bone et al., 2014). High-energy resolution fluorescence-detected XANES (HERFD-XANES) has been developed to further enhance the capability of XANES in Hg speciation (Proux et al., 2017), which could reveal the chemical state and bonding environment of Hg at concentrations even as low as 1 mg Hg/kg (Manceau et al., 2016; Vogel et al., 2016). For most environmental samples, e.g. uncontaminated soil and sediment, the Hg concentration is usually lower than 1 mg Hg/kg, which requires further development in the detection limit of XAFS.

XRD is widely used in identifying the crystalline phase of crystalline material (Selvaraj et al., 2014). Its detection limit is about 2% HgS (W/W), limiting its application in the natural environmental samples with low Hg concentration. XRD has been applied in the identification and differentiation of α-HgS and β-HgS. It also has been used to identify the nanoparticles generated in the Hg-S-DOM system and confirm that the products were HgS NPs with poor crystallinity (Pham et al., 2014). Small-angle X-ray scattering (SAXS) could give information on primary particle size, morphology, as well as interactions between particles (Li et al., 2016b). Combined with DLS, SAXS has been used to study the size of HgS NPs during aging in the presence of DOM, and the results showed that the monomer particles agglomerated to form large aggregates during the aging, but the size of the primary monomer particles remains unchanged, indicating that the aggregation of nanoparticles during the aging process is an interaction between particles (Pham et al., 2014).

Table 1 – Summary of analytical techniques for HgS NPs.

Techniques	Functions	Sample requirement or detection limit	Characteristics	Applications	Refs.
Scanning electron microscope (SEM); Transmission electron microscope (TEM)	Microstructure, morphology, and crystal structure TEM-SAED and TEM-EDX: crystallographic and elemental composition	Solid sample: weight > 0.02 g; Dispersion sample needs to be deposited on the copper mesh SEM: requires conductive samples; TEM: requires thin samples	Artifacts may be introduced during sample preparation; samples are prone to change or damage after exposure to electron beams Only a small part of the sample can be detected Searching for the target may take a lot of time	SEM/TEM-EDX and SEM/TEM-SAED were used to detect nano-scale and micro-scale HgS in soils, minerals, plant leaves, and roots, human tissue, and medicine, indicating the presence of HgS NPs in the environment	Barnett et al. (1997), Kocman et al. (2011), Satake et al. (1990), Yan (2007), Janadri et al. (2015)
X-ray photoelectron spectroscopy (XPS)	Element composition and content, molecular structure, and chemical bond	Powder sample: thickness < 2 mm Requiring conductive samples	Non-destructive technique	XPS was used to detect nano- and micro-HgS crystals in soils and aquatic bryophyte cells	Satake et al. (1990), Barnett et al. (1997), Kocman et al. (2011)
Dynamic light scattering (DLS)	Hydrodynamic particle size distribution of nanoparticles in suspension	Detection limit > 1 mg/L(Hg)	Test results could be disturbed by environmental colloids such as clay and biological debris Providing the hydrodynamic size calculated based on the movement of the particles in the solution The result tends to be the hydrodynamic particle size of large particles, which cannot represent the average level of particles in the solution	TEM and DLS were used to study the generation and aggregation of HgS NPs in the Hg-S-DOM system. Results showed that HgS NPs with a particle size of 3-5 nm were formed in the system. The particles aggregate during the aging, but the primary particle size remains the same	Pham et al. (2014)
Ultraviolet-visible spectroscopy (UV-Vis)	Nanoparticle size in suspension	Requires nanoparticle dispersion	The particle size is indirectly judged by observing the valence electron transition band gap, and the quantitative relationship is affected by the experimental system	UV-Vis, TEM, and DLS were used to study the growth process of HgS NPs in the Hg-S-DOM system. The average particle size of HgS NPs measured by UV-Vis (5.4 ± 0.02 nm) was similar to the result measured by TEM (7.5 ± 1.5 nm)	Slowey (2010)

(*continued on next page*)

Table 1 (*continued*)

Techniques	Functions	Sample requirement or detection limit	Characteristics	Applications	Refs.
X-ray diffraction (XRD)	Element composition and content, molecular structure, and chemical bond	Powder sample: weight >5 mg Detection limit: 2% HgS (w/w)	Insensitive to non-crystalline particles, the presence of non-crystalline particles in the environmental samples may be underestimated	XRD was used to study the particles generated in the Hg-S-DOM system, confirming that the products were HgS NPs with poor crystallinity (about 10 nm)	Pham et al. (2014)
Extended X-ray absorption fine structure (EXAFS)	The number, type, and proximity of atoms adjacent to the Hg element	Detection limit >100 mg/kg(Hg)	Non-destructive analysis High specificity The samples are required to have a high Hg concentration	EXAFS was used to study the effect of DOM on the formation of HgS NPs. Results showed that HgS NPs generated in the presence of DOM had lower coordination numbers and shorter atomic distances, indicating that DOM can not only limit the size of HgS particles to the nanoscale but also can lead to an increase in the degree of disorder	Slowey (2010), Combes et al. (1989), Frenkel et al. (2001)
Small-angle X-ray scattering (SAXS)	Primary particle size, shape, and distribution	Measuring the structure characteristics of particles in the range of 1-1000 nm Suitable for sparse systems	There may appear interference to scattered intensities	SAXS and DLS were used to study the size of HgS NPs during aging in the presence of DOM. Results showed that the monomer particles agglomerated to form large aggregates during the aging, but the size of the primary monomer particles remains unchanged, indicating that the aggregation of nanoparticles during the aging process is an interaction between particles	Pham et al. (2014)
Single-particle inductively coupled plasma mass spectrometry (SP-ICP-MS)	Number of particles, particle size, and particle size distribution	Detection limit < 10^5 pcs / mL (Particle number); particle size >10 nm	The elemental composition of nanoparticles could not be identified	SP-ICP-MS was used to quantify indigenous Hg-NPs in natural soils as well as the liver and muscle of cetaceans, the results were confirmed by TEM-EDX. AF4-UV-MALS-ICP-MS/MS was used to detect the composition of nanoparticles in petroleum hydrocarbon condensate, and analytical results were confirmed by TEM-EDX and SP-ICP-MS.	Cai et al. (2022), Ji et al. (2022), Ruhland et al. (2019)

Quantitative analysis of HgS NPs is mainly achieved by atomic fluorescence spectrometry (AFS) and SP-ICP-MS, showing the quantitative levels of HgS NPs in the samples. Extracting HgS NPs from environmental matrices is the first and critical step for further instrumental quantification. A wide range of techniques has been used to extract nanoparticles from complex matrices, including dispersant extraction, chromatographic separation, centrifugal separation, ultrafiltration separation, and field flow classification (Bundschuh et al., 2018). Selection of the extraction methods mainly depends on the average particle size, size distribution, surface characteristics, shape, and chemical composition of the target particle (Bundschuh et al., 2018). Filtration (e.g., using 0.22 μm membrane) and ultracentrifugation (e.g., 370,000 g for 2 hr) have been applied to separate HgS NPs from natural organic matter dissolution and interstitial water, and the concentration of HgS NPs is then quantified by AFS (Zhang et al., 2012, 2014).

Single particle inductively coupled plasma-mass spectrometry (SP-ICP-MS) could discriminate particulate and dissolved forms of Hg in environmental samples and offers simultaneous information on particle number/mass concentrations and size distribution. It is an effective method for the analysis of liquid samples and has been widely used in the quantification of nanoparticles such as $Ag^{(0)}$ NPs, ZnO NPs, and TiO_2 NPs (Flores et al., 2021; Mozhayeva and Engelhard, 2020). Due to the shortage in analysis elemental composition of nanoparticles, SP-ICP-MS is usually combined with other techniques, e.g., TEM-EDX. Recently, a standardized protocol, by using tetrasodium pyrophosphate (TSPP) for extraction and SP-ICP-MS for quantification, has been developed to quantify Hg-containing nanoparticles (Hg-NPs) in different natural soils, and the results showed that indigenous Hg-NPs in these selected soils were within 10^7-10^{11} NPs /g, accounting for 3%-40% mass basis of THg, which contributed to 5%-65% of the measured MeHg in soils (Cai et al., 2022). With the help of size exclusion chromatography coupled with inductively coupled plasma (SEC-ICP-MS), TEM, and SP-ICP-MS, large amounts (9-161 mg/kg) of Hg-NPs have been observed in the liver and muscle of cetaceans (Ji et al., 2022). Besides, asymmetric flow field flow fractionation ICP MS/MS (AF4-ICP-MS/MS) has been used to detect the occurrence of natural HgS NPs (with the diameter range of 15 - 400 nm) in petroleum hydrocarbon condensate, and the results were confirmed by STEM-EDX and SP-ICP-MS (Ruhland et al., 2019).

More delicate methods for extracting HgS NPs from complex matrices (e.g., soils or sediments) are needed to ensure that the size, form, and aggregation state of nanoparticles keep unchanged during the extraction. It is also critical to optimize instrumental parameters to improve the sensitivity and limit of detection (LOD), which would help to obtain more accurate data.

Though several methods have been developed for the identification and quantification of HgS NPs, challenges still exist in detecting their presence and measuring their concentrations in environmental and biological samples. Most of these methods are time-consuming and require sample pretreatment, possibly changing the size or shape of HgS NPs and introducing analytical artifacts. It calls for more cost-effective detection and non-destructive methods to help further explore the presence and stock of HgS NPs in the environment.

2.2. *HgS NPs in the environment and organisms*

HgS NPs have been widely detected in various environmental matrices (e.g., soils, marshes, and minerals), organisms, traditional medicines, and even human body fluids (Fig. 2, Table 2) (Barnett et al., 1997; Liu et al., 2020; Lowry et al., 2004; Lu et al., 2020; Patty et al., 2009). Barnett et al. (1997) first found there were submicron β-HgS crystal grains (with a particle size of 20-100 nm) in the form of metacinnabar in the Oak Ridge floodplain wetland in Tennessee, USA. Liu et al. (2020) observed the presence of HgS NP crystals and found that they aggregated with different shapes and sizes in Hg-contained pyrite samples from a gold mine. It is believed that both natural (e.g., oxidation and fracture) and industrial processes (e.g., roasting and smelting) can decompose host minerals, thereby releasing HgS NPs into the environment. Patty et al. (2009) speculated *Spartina* cordgrass could transform Hg^{2+} into HgS NPs, as HgS NPs were observed in the root tissues and root surface of native *Spartina foliosa*. Manceau et al. (2018) first observed the *in vivo* formation of HgS NPs in intact leaves, providing evidence for the widespread presence of HgS NPs in oxygenated environment. The aerial gaseous Hg (i.e., Hg^0) taken up by leaf tissues can be sequestered as HgS NPs as much as 57%. Wu and Wang (2014) found that HgS NPs were an important inorganic Hg species in marine microalgae cells (*Chlorella autotrophica, Isochrysis galbana*, and *Thalassiosira weissflogii*), accounting for 20%-90% of the total Hg in cells.

Moreover, HgS NPs may enter the human body via dietary exposure, raising health concerns. HgS particles of various sizes, including HgS NPs, are an important component of some Asian traditional medicines (Li et al., 2021). HgS NPs have been widely detected in Traditional Tibetan Medicines (e.g., *Zuotai*) (Li et al., 2016a; Yan, 2007), Ayurveda drug (e.g., *Shwas kuthar rasa, Ras-Sindoor, Poorna Chandrodaya Chenduram*, and *Linga Chenduram*), and Siddha drug (e.g., *linga chenduram* and *Poorna chandrodayam*were) (Al-Ansari et al., 2021; Arun et al., 2009; Austin, 2012; Janadri et al., 2015; Mukhi et al., 2017; Singh et al., 2009). It is necessary to consider the assimilation rate of large-particle HgS and HgS NPs in the human body due to the difference in the activity, which would help understand the therapeutic effects and toxicity of HgS-containing medicines. Chemical forms of metals in different traditional medicines are a major determinant in assessing their disposition, efficacy, and toxicity (Liu et al., 2019). To further assess the amount of Hg in these medicines that are bioavailable to the human body and thus associated health risk of Hg, more investigations are required for the analysis of chemical formulae and histopathological studies on these medicines, which could also improve our understanding of HgS and HgS NP toxicity. Furthermore, HgS NPs are also detected in human fluids. Lu et al. (2020) firstly detected HgS NPs in the pleural effusion of non-occupationally exposed people in Pearl River Delta, China. This study provides preliminary evidence for the potential health risks of HgS NPs, while the transformation, dissolution, and toxic effects of HgS NPs in the human body

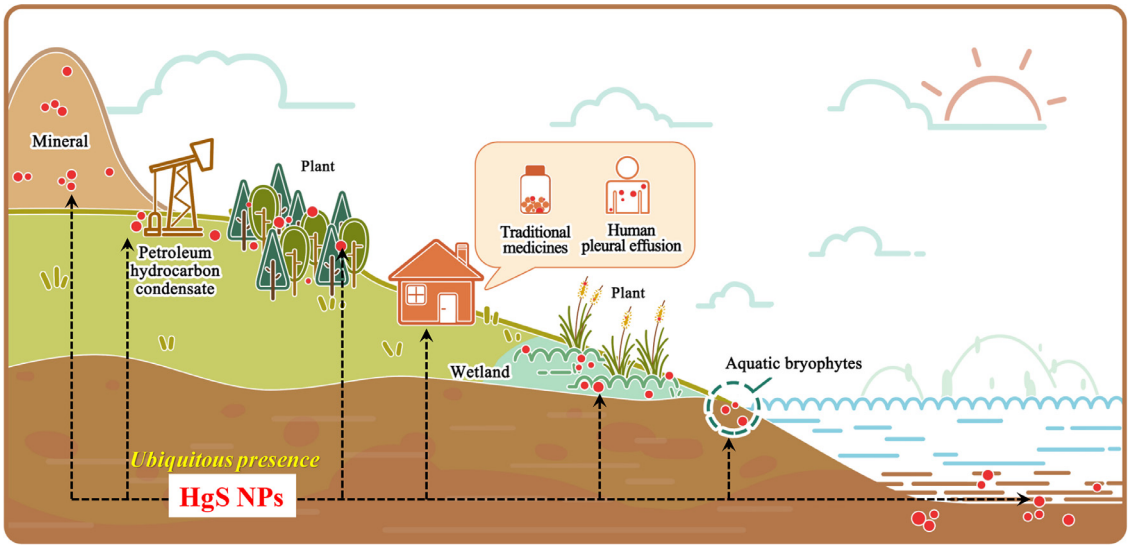

Fig. 2 – A conceptual figure showing the ubiquitous presence of HgS NPs in natural environment and organisms. The red dots represent the occurrence of HgS NPs, which have been widely detected in various environmental matrices (e.g., soils, marshes, and minerals), organisms, traditional medicines, and even human body fluids. The contents of this figure were summarized from previous studies (Table 2).

and their relationship with diseases have not been fully explored yet.

3. DOM alters the environmental behaviors of HgS NPs

DOM comprising the partial decomposition products of plants and other biological materials is ubiquitous in natural environment (Jiang et al., 2020; Roth et al., 2019; Zark and Dittmar, 2018). DOM has long been known to contain many metal-binding functional groups (Li and Gong, 2021), such as carboxyl group (R-COOH), phenolic hydroxyl group (Ar-OH), alcoholic hydroxyl group (R-OH), methoxy group (R-OCH_3), and aldehyde group (R-CHO), which would help DOM bind with nanoparticles and affect their surface chemistry, aggregation process, and dissolution process (He et al., 2016; Li et al., 2020; Philippe and Schaumann, 2014). The interactions between DOM and nanoparticles will collectively determine the persistence and bioavailability of nanoparticles to organisms (Aiken et al., 2011).

The process of Hg methylation is believed to be an intracellular reaction (Gilmour et al., 2011; Parks et al., 2013), and the microbial uptake pathways determine the bioavailability of HgS NPs for microbial Hg methylators (Hochella Michael et al., 2008). Presumably, HgS NPs may be absorbed by microorganisms directly as nanoparticles or Hg^{2+} after being dissolved. DOM has been proposed to interact with HgS NPs and affect its microbial methylation (Graham et al., 2012). Considering the various sources, complex structure, and different functional composition, DOM can affect the environmental behaviors and bioavailability of HgS NPs in different ways: (1) influencing the extent of structural order of HgS NPs, (2) participating in the dissolution of HgS NPs, (3) regulating the aggregation of HgS NPs, and (4) changing the surface properties of HgS NPs (Fig. 3).

3.1. *DOM influences the structural order of HgS NPs*

Disordered HgS NPs were more bioavailable for microbial Hg methylators (Pham et al., 2014), which could be attributed to their increased surface reactivity and faster dissolution rates (Hochella et al., 2008; Poulin et al., 2017). DOM has been proved to inhibit the precipitation of HgS NPs and significantly limit the extent of structural order of HgS NPs. The inhibition of HgS precipitation in aqueous solutions could be ascribed to the complexation of strong DOM-Hg binding (Ravichandran et al., 1999), resulting in a limited structural order of HgS NPs. DOM with greater aromaticity favored the formation of smaller and more disordered β-HgS NPs (Poulin et al., 2017; Slowey, 2010), as evaluated by the Hg-S coordination number and interatomic Hg-S distance (Gerbig et al., 2011). The abundant aromatic biomolecules in EPS derived from bacteria have been found to enhance the short-range structural disorder of HgS NPs via inner-sphere complexation and consequently increase the bioavailability of nanoparticulate Hg (i.e., promoting its microbial methylation) (Zhang et al., 2020). It is necessary to pay more attention to the sources and compositions of DOM to understand their impacts on the behaviors of HgS NPs (Pham et al., 2014). Besides, geochemical factors that control the structural order of HgS NPs (e.g., the sulfide concentration, Hg^{2+}: DOC ratio, or kinetics of Hg^{2+}-DOM-sulfide interactions) (Pham et al., 2014; Poulin et al., 2017) should be further explored.

3.2. *DOM participates in the dissolution of HgS NPs*

The dissolution of nanoparticles refers to the process of releasing water-soluble ions or molecules from nanoparticles,

Table 2 – Reports of HgS NP detection in natural environment and organisms.

Environmental matrices		Main findings	Refs.
Wetland soil		Submicron Hg sulfide crystals (β-HgS) with a particle size of 50-100 nm were observed in Hg-contaminated soils in the floodplain of Oak Ridge, Tennessee, USA, proving the evidence that HgS NPs could naturally exist in soils	Barnett et al. (1997)
Sediment		Half of the Hg in the <0.5 μm size fraction of contaminated marine sediment existed as individual HgS NPs (β-HgS) based on the analysis of single-particle inductively coupled plasma time-of-flight mass spectrometry and XAS	Xu et al. (2021)
Mineral	Tailings	HgS particles were observed in Hg tailings particles and their calcined products, with a particle size of ~500 nm, which proved that colloidal particles of HgS are the main form of Hg species in these mine wastes	Lowry et al. (2004)
	Pyrite	HgS NPs were observed in pyrrhotite samples with a particle size of 5-30 nm	Liu et al. (2020)
Petroleum		HgS NPs were observed in petroleum hydrocarbon condensate with a particle size of 15-195 nm	Ruhland et al. (2019)
Plant	Aquatic bryophyte	Single crystal HgS particles (5-15 nm) and polycrystalline HgS particles (10-200 nm) were observed in the cell walls of *Jungermannia vulcanicola* Steph. and *Scapania undulata* (L.) Dum., proving the existence of HgS NPs in plants	Satake et al. (1990)
	Higher plant root and leaves	Hg nanoparticles and hexagonal crystals were observed in the root tissues of native *Spartina foliosa*. XANES showed that the Hg-S bonding structure was similar to α-HgS and β-HgS, which might be HgS NPs. HgS nanoparticles (3-5 nm) were observed in the leaves of 22 native plants of 6 different species from Wuchuan and Wanshan, Guizhou, confirming the presence of HgS NPs in the oxygen-containing environment	Manceau et al. (2018), Patty et al. (2009)
Mammal	Human pleural effusion	Exogenous HgS NPs were observed in the human pleural effusion	Lu et al. (2020)
	Cetacean liver and muscle	Natural HgS NPs were identified in both liver and muscle of cetaceans	Ji et al. (2022)
Traditional medicine	Traditional Tibetan Medicines	*Zuotai* contained HgS NPs (100~800 nm) composed of β-HgS and α-HgS	Li et al. (2016a), Yan (2007)
	Ayurveda and Siddha drug	Ayurveda: *Shwas kuthar rasa, Ras Sindoor, Rasasindur,* and *Poorna Chandrodaya Chenduram* were confirmed to contain HgS NPs within the diameter of 31-56 nm, 25-50 nm, 8-16 nm, respectively Siddha: *Linga Chenduram* and *Poorna chandrodayam*were confirmed to contain HgS NPs within the diameter of ~500 nm and 60-70 nm, respectively	Al-Ansari et al. (2021), Arun et al. (2009), Austin (2012), Janadri et al. (2015), Mukhi et al. (2017), Singh et al. (2009)

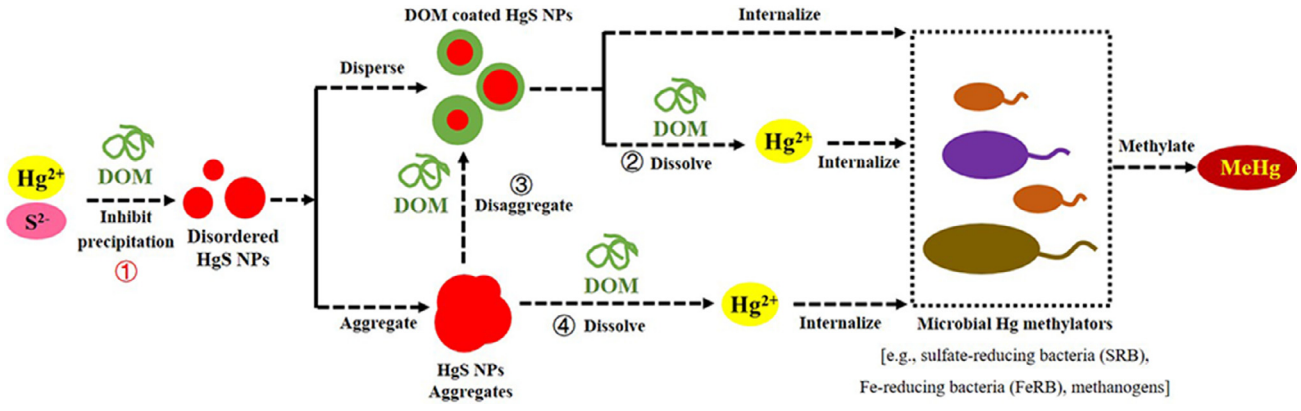

Fig. 3 – A schematic diagram showing how DOM alters the environmental behaviors of HgS NPs and their bioavailability. ① DOM inhibits the precipitation of HgS NPs and limits the structural order in HgS NPs; ② DOM participates in the dissolution of HgS NPs; ③ DOM regulates the aggregation of HgS NPs; ④ DOM changes the surface properties of HgS NPs.

which is an important chemical transformation process of nanoparticles in the environment (Abbas et al., 2020). The dissolution rate (solubility kinetics) and extent (solubility balance) depend on their intrinsic properties (e.g., chemical composition, coating or surface chemistry, crystalline phase, morphology, size, and surface area) and environmental conditions (e.g., pH, ionic strength, redox potential, temperature, inorganic ligands, light, and DOM) (Amde et al., 2017; Misra et al., 2012).

DOM could mediate the dissolution of HgS and HgS NPs through complexation reactions, which may largely be affected by their characteristics (Mohd Omar et al., 2014; Ravichandran et al., 1999; Slowey, 2010). DOM is easily adsorbed to the surface of HgS and promotes some changes in the micro-environment around the Hg atom, causing the break of the Hg-S bond. Subsequently, Hg (possibly as a Hg-DOM complex), is released into solution (Waples et al., 2005). The HgS dissolution rate in different DOM solutions was proved to be positively correlated with the specific ultraviolet absorbance, aromaticity, and molecular weight of DOM (Waples et al., 2005). According to a recent study, EPS of *D. desulfuricans* ND132 could hardly accelerate the dissolution of HgS NPs (Zhang et al., 2020). However, considering the dissolution rate of HgS may depend on the sites or functional groups of DOM that bind Hg (Louie et al., 2013), it is necessary to investigate the effects of other DOM components on the dissolution of HgS NPs. Besides, it should be noted that the enhanced dissolution of HgS in the presence of DOM may include both dissolved Hg^{2+} (generally as Hg^{2+}-DOM complex) and DOM-dispersed HgS NPs (which can easily penetrate 0.1 μm filter membranes), both of which are generally defined as "dissolved Hg fraction" (Pham et al., 2014). When evaluating the methylation of HgS NPs under the influence of DOM, it is necessary to distinguish the contributions of Hg^{2+} and HgS NPs to Hg bioavailability, which could help us further understand their roles in the Hg methylation.

More importantly, the reduction reaction may also regulate the dissolution and fate of HgS NPs. A recent study showed that about 45% of HgS NPs (3–5 nm) could be reduced by *Geobacter sulfurreducens* PCA (a typical strain of iron reduction bacteria) into highly active Hg^0 in 0.5 hr, which is much higher than the reduction efficiency for Hg^{2+}-DOM solution (~4%) (Cui, 2021). Thigh reduction rate may be attributed to the reaction activity of nanoparticles, e.g., higher adsorption capacity and dissolution rate. It was also found that the reduction of HgS NPs decreased with prolonged aging and increased particle size, suggesting the crystal structure and particle size played important roles in the reduction process. Notably, about 3% of the HgS NPs aged for 4 years could also be reduced, implying the reduction potential of HgS NPs existing in natural environment (Cui, 2021). It is hypothesized that DOM may participate in the dissolution of HgS NPs, e.g., absorbed to the surface of HgS NPs, and regulate their reduction process, although the molecular regulation mechanism in reduction need to be further explored.

3.3. *DOM regulates the aggregation of HgS NPs*

Nanoparticles tend to aggregate into clusters through homogeneous aggregation (with themselves) or heterogeneous aggregation (with natural minerals and organic colloids) (Lei et al., 2018), which would change their mobility, reactivity, and potential toxicity in the environment (Batley et al., 2013; Dwivedi et al., 2015). Many studies have emphasized the prominent effect of DOM on the properties and behaviors of nanoparticles (Philippe and Schaumann, 2014). DOM is adsorbed onto the surface of nanoparticles and affects the stability of nanoparticles through steric hindrance, electrostatic repulsion, electrical neutralization, bridging, and patch charge (Maurer-Jones et al., 2013). The effects of DOM on the stabilization or aggregation of nanoparticles depend on the properties of DOM, nanoparticles, and the environmental conditions (pH, ionic strength, and cations) (Philippe and Schaumann, 2014).

It has been proved that the adsorption of negatively charged DOM on the β-HgS NP surface could enhance electrostatic repulsive forces and induce electrostatic forces, hindering the aggregation of β-HgS NPs (Deonarine and Hsu-Kim, 2009; Gerbig et al., 2011; Philippe and Schaumann, 2014; Ravichandran et al., 1999; Slowey, 2010). Hydrophobic organic acids (humic and fulvic acids) showed more inhibitory effects on the aggregation of β-HgS NPs than hydrophilic organic acids (Ravichandran et al., 1999). Besides, aromatic DOM also plays an important role in inhibiting the aggregation of HgS NPs. Zhang et al. (2020) proposed that the abundant aromatic biomolecules in EPS can interact strongly with HgS NPs through inner complexation, thereby inhibiting the aggregation of HgS NPs. Besides, the adsorption of DOM on the agglomerates could increase the surface charge and repulsive forces and thus become dominant within the matrix, followed by the agglomerates rupture (Baalousha et al., 2008). Suwannee River Humic Acid (SRHA) and alginate have been found to disaggregate FeO NPs (Baalousha et al., 2008), TiO_2 NPs (Loosli et al., 2013), ZnO NPs agglomerates (Mohd Omar et al., 2014), future studies should highlight the DOM impacted disaggregation of HgS NPs.

Besides, other environmental factors, e.g., light, could also impact the nanoparticles and DOM-nanoparticles complexes, which would make the system more complicated (Das et al., 2012). For instance, Poda et al. (2013) observed that light can induce the oxidation and dissolution of the polyvinylpyrrolidone (PVP) coated on the Ag NP surface, thereby changing the stability and size of the particles. Mazrui et al. (2018) observed light-accelerated aggregation and sedimentation of DOM stabilized β-HgS NPs, which could be attributed to the photochemical reaction of HgS NPs induced by light or the photooxidation of organic matter coated on the surface of β-HgS NPs. The effects of other multiple environmental factors on DOM adsorbed to the surface of HgS NPs and the effects on the fate of the HgS NPs, have not been fully investigated.

The role of DOM in the HgS NP stabilization/agglomeration in natural environment largely relies on the sources, intrinsic properties, and environmental conditions (Abbas et al., 2020). Natural surface water contains a mixture of all DOM types (Yan et al., 2019), and thus it is difficult to identify the dominant component of DOM interacting with colloids. Thorough characterization of DOM by Fourier-transform ion cyclotron resonance (FT-ICR MS), e.g., the molecular weight and the molecular structure including the configuration of reactive groups (Kellerman et al., 2018; Lei et al., 2021b), will help elucidate adsorption mechanisms of DOM on HgS NPs and under-

stand the competition between different types of DOM (e.g., humic substances, polysaccharides, proteins, and fatty acids) for the adsorption on HgS NP surfaces.

3.4. *DOM changes the surface properties of HgS NPs*

The adsorption or coating of DOM on nanoparticles surfaces could regulate the surface properties of HgS NPs through changing the crystal structure and imparting electrostatic and steric hindrances, consequently impacting the nanoparticles-organisms interaction and changing the bioavailability of HgS NPs to organisms (Tian et al., 2021a; Yu et al., 2018). The crystal structure of nanocrystals determines the physical and chemical properties of nanoparticles, which is critical for understanding the environmental behavior of nanoparticles (Fan and Zhang, 2016; Tian et al., 2021a, 2021b; Yan et al., 2017). DOM is a powerful tool to tailor nanocrystal shapes. The relative energy of the crystal facets can be varied exploiting crystallographically selective adhesion of DOM (Jun et al., 2003). Tian et al. (2021a) first proved that the exposed crystal facet is a crucial parameter for determining the microbial methylation potential of HgS NPs. The (111) facet of HgS NPs has the highest affinity to the microbial Hg methylators due to the favored binding of metacinnabar (111) facet with metal transporters on cell surfaces, which makes this facet relatively more bioavailable. Natural ligands, e.g., DOM, could protect the (111) facet from diminishing during nanocrystal growth through preferential adsorption and consequently hinder the mercury methylation of HgS NPs from natural attenuation. The results indicated that preferential binding between ligand-rich molecules and fast-formed crystal faces may be a natural tool for tailoring the crystal structure and tuning the bioavailability of reactive mineral phases, which further emphasized the importance of DOM in tailoring the surface properties of HgS NPs (Tian et al., 2021a).

While some results have suggested that DOM has dual effects on the toxicity and bioavailability of nanoparticles. Firstly, DOM could hinder the adhere of nanoparticles onto cell membranes and decrease the toxicity and bioavailability of nanoparticles (Liang et al., 2020). Low molecular weight DOM could afford electrostatic repulsions while large uncharged polymers could hamper the adhesion of nanoparticles to cell surfaces by steric repulsions (Yu et al., 2018). Secondly, some organic matter coatings would increase the number of cell membrane receptors that can “recognize” the nanoparticles, especially for proteins, and thereby increase the nanoparticle internalization rate (Liang et al., 2020). These results indicated that the surface properties and bioavailability of HgS NPs would be altered under the regulation of different DOM types when transporting in the environment. More attention should be paid to the characteristics of DOM (e.g., molecular weight, aromaticity, and hydrophobicity), which determines the relationship between DOM and HgS NPs.

In addition to DOM, some other factors may also impact the environmental behaviors of HgS NPs, such as the particle size of nanoparticles and microorganism species. The size of nanoparticles is essential to the Hg methylation potential, e.g., higher methylation (6%-10%) was observed in smaller HgS NPs (3-4 nm) when compared with larger particles (0.13% methylation, within 500 nm) (Zhang et al., 2014). Besides, there may be differences in the uptake and Hg methylation of HgS NPs by different microbial species. For instance, in the cultures of *D. desulfuricans* ND132, the methylation potential of HgS-EPS nanoparticles was significantly higher when compared with HgS NPs formed without EPS. Nevertheless, HgS NPs formed with or without the EPS of *G. sulfurreducens* PCA showed no differences in the bioavailability (Zhang et al., 2020). It should be noted that there is still no direct evidence showing that nanoparticles could be taken up by microbial Hg methylators (Dehner et al., 2011), and it is speculated this process would likely be dependent on the sizes of nanoparticles and species of microorganisms.

4. Outlook

Studies have demonstrated that HgS NPs could be the predominant source of MeHg that causes environmental risks. To better understand the risks of HgS NPs, further research is required on the field observations of HgS NPs and the impacts of DOM on the transfer, transformation, and bio-absorption of HgS NPs under environmentally relevant concentrations. Future research priorities may be given to the following directions:

(1) *Further improving methods for detecting HgS NPs in complex matrices*
Developing sensitive and non-destructive methods for size characterization and mass/number quantification of HgS NPs and the structure of HgS NP aggregates would help further understand the biogeochemical cycling and toxicity of HgS NPs. HgS NPs have been identified in soils, sediment, minerals, plants, microalgae, and bacteria, while their general presence in the environment and biosphere remains to be explored, which is being hindered by the limitations in the sensitivity of analytical methods. Besides, HgS NPs have been demonstrated to be available for microbial Hg methylators, while the mechanisms and pathways for the uptake of HgS NPs by microorganisms remain unclear. Further improvement of analytical methods/technologies, e.g., with higher spatial resolution and sensitivity, are urgently required to support the studies on the uptake and transport pathways of HgS NPs into microorganisms, which will benefit better understanding the bioavailability and toxicity of HgS NPs.

(2) *Better understanding the interactions between DOM and HgS NPs*
Currently, the complex interactions between DOM and HgS NPs are far from clear, partly due to the heterogeneity of natural organic matter. Firstly, better revealing characteristics of DOM (e.g., molecular weight and molecular structure including the configuration of reactive groups) with advanced techniques could help interpret the adsorption mechanisms of DOM onto HgS NPs. Secondly, the identification and quantification of the functional groups of DOM that exhibit a strong binding capability to HgS NPs and understanding the configuration and stereo chemistries of DOM that influence its adsorption onto HgS NPs would help understand and predict the fate of DOM-coated HgS NPs. Besides, natural surface water contains a mixture of

different types of DOM. Further attention should be paid to the competition among various DOM types for sorption on the HgS NP surface, which could facilitate identifying the key DOM components that govern the fates of HgS NPs in natural environment.

Acknowledgments

This work was supported by the Natural Science Foundation of Jiangsu Province (No. BK20200322), the National Natural Science Foundation of China (Nos. 42107383, U2032201), and the special fund from the State Key Joint Laboratory of Environment Simulation and Pollution Control (RCEES, CAS) (No. 20K02ESPCR).

REFERENCES

Abbas, Q., Yousaf, B., Amina, Ali, M.U., Munir, M.A.M., El-Naggar, A., et al., 2020. Transformation pathways and fate of engineered nanoparticles (ENPs) in distinct interactive environmental compartments: a review. Environ. Int. 138, 105646.

Aiken, G.R., Hsu-Kim, H., Ryan, J.N., 2011. Influence of dissolved organic matter on the environmental fate of metals, nanoparticles, and colloids. Environ. Sci. Technol. 45, 3196–3201.

Aiking, H., Govers, H., van't Riet, J., 1985. Detoxification of mercury, cadmium, and lead in *Klebsiella aerogenes* NCTC 418 growing in continuous culture. Appl. Environ. Microbiol. 50, 1262–1267.

Al-Ansari, M.M., Ranjit Singh, A.J.A., Al-Khattaf, F.S., Michael, J.S., 2021. Nano-formulation of herbo-mineral alternative medicine from linga chenduram and evaluation of antiviral efficacy. Saudi J. Biol. Sci. 28, 1596–1606.

Amde, M., Liu, J., Tan, Z., Bekana, D., 2017. Transformation and bioavailability of metal oxide nanoparticles in aquatic and terrestrial environments. A review. Environ. Pollut. 230, 250–267.

Arun, S., Murty, V.S., Chandra, T.S., 2009. Standardization of metal-based herbal medicines. Am. J. Infect. Dis. 5, 193–199.

Austin, A, 2012. Chemical characterization of a gold and mercury based siddha sasthric preparation-*poorna chandrodayam*. Am. J. Drug Discov. Dev. 2, 110–123.

Baalousha, M., Manciulea, A., Cumberland, S., Kendall, K., Lead, J.R., 2008. Aggregation and surface properties of iron oxide nanoparticles: influence of pH and natural organic matter. Environ. Toxicol. Chem. 27, 1875–1882.

Barnett, M.O., Harris, L.A., Turner, R.R., Stevenson, R.J., Henson, T.J., Melton, R.C., et al., 1997. Formation of mercuric sulfide in soil. Environ. Sci. Technol. 31, 3037–3043.

Batley, G.E., Kirby, J.K., McLaughlin, M.J., 2013. Fate and risks of nanomaterials in aquatic and terrestrial environments. Acc. Chem. Res. 46, 854–862.

Benoit, J.M., Gilmour, C.C., Mason, R.P., Heyes, A., 1999. Sulfide controls on mercury speciation and bioavailability to methylating bacteria in sediment pore waters. Environ. Sci. Technol. 33 (6), 951–957.

Bone, S.E., Bargar, J.R., Sposito, G., 2014. Mackinawite (FeS) reduces mercury(II) under sulfidic conditions. Environ. Sci. Technol. 48 (18), 10681–10689.

Bravo, A.G., Cosio, C., 2020. Biotic formation of methylmercury: A bio–physico–chemical conundrum. Limnol. Oceanogr. 65, 1010–1027.

Bundschuh, M., Filser, J., Lüderwald, S., McKee, M.S., Metreveli, G., Schaumann, G.E., Schulz, R., Wagner, S., 2018. Nanoparticles in the environment: where do we come from, where do we go to? Environ. Sci. Eur. 30, 6.

Cai, W., Wang, Y., Feng, Y., Liu, P., Dong, S., Meng, B., et al., 2022. Extraction and quantification of nanoparticulate mercury in natural soils. Environ. Sci. Technol. 56, 1763–1770.

Chen, L., Liang, S., Liu, M., Yi, Y., Mi, Z., Zhang, Y., et al., 2019. Trans-provincial health impacts of atmospheric mercury emissions in China. Nat. Commun. 10, 1484.

Chen, Y., Yin, Y., Shi, J., Liu, G., Hu, L., Liu, J., et al., 2017. Analytical methods, formation, and dissolution of cinnabar and its impact on environmental cycle of mercury. Crit. Rev. Environ. Sci. Technol. 47, 2415–2447.

Clever, H.L., Johnson, S.A., Derrick, M.E., 1985. The solubility of mercury and some sparingly soluble mercury salts in water and aqueous electrolyte solutions. J. Phys. Chem. Ref. Data. 14, 631–680.

Cui, Y., 2021. Monitoring and mechanism analysis of microbial reduction process of HgS nanoparticles. Jianghan University, Wuhan, China (in Chinese).

Combes, J.M., Manceau, A., Calas, G., Bottero, J.Y., 1989. Formation of ferric oxides from aqueous solutions: A polyhedral approach by X-ray absorption spectroscdpy: I. Hydrolysis and formation of ferric gels. Geochim. Cosmochim. Acta 53, 583–594.

Das, P., Williams, C.J., Fulthorpe, R.R., Hoque, M.E., Metcalfe, C.D., Xenopoulos, M.A., 2012. Changes in bacterial community structure after exposure to silver nanoparticles in natural waters. Environ. Sci. Technol. 46, 9120–9128.

Dehner, C.A., Barton, L., Maurice, P.A., Dubois, J.L., 2011. Size-dependent bioavailability of Hematite (*alpha*-Fe_2O_3) nanoparticles to a common aerobic bacterium. Environ. Sci. Technol. 45 (3), 977–983.

Deonarine, A., Hsu-Kim, H., 2009. Precipitation of mercuric sulfide nanoparticles in NOM-containing water: implications for the natural environment. Environ. Sci. Technol. 43, 2368–2373.

Dong, W., Liu, J., Wei, L., Yang, J., Chernick, M, Hinton, D.E., 2016. Developmental toxicity from exposure to various forms of mercury compounds in medaka fish (*Oryzias latipes*) embryos. PeerJ 4, e2282.

Drott, A., Björn, E., Bouchet, S., Skyllberg, U., 2013. Refining thermodynamic constants for mercury(II)-sulfides in equilibrium with metacinnabar at sub-micromolar aqueous sulfide concentrations. Environ. Sci. Technol. 47 (9), 4197–4203.

Dwivedi, A.D., Dubey, S.P., Sillanpää, M., Kwon, Y.N., Lee, C., Varma, R.S., 2015. Fate of engineered nanoparticles: implications in the environment. Coord. Chem. Rev. 287, 64–78.

Enescu, M., Nagy, K.L., Manceau, A., 2016. Nucleation of mercury sulfide by dealkylation. Sci. Rep. 6, 39359.

Fan, Z., Zhang, H., 2016. Crystal phase-controlled synthesis, properties and applications of noble metal nanomaterials. Chem. Soc. Rev. 45, 63–82.

Flores, K., Turley, R.S., Valdes, C., Ye, Y., Cantu, J., Hernandez-Viezcas, J.A., et al., 2021. Environmental applications and recent innovations in single particle inductively coupled plasma mass spectrometry (SP-ICP-MS). Appl. Spectrosc. Rev. 56, 1–26.

Frenkel, A.I., Hills, C.W., Nuzzo, R.G., 2001. A view from the inside: complexity in the atomic scale ordering of supported metal nanoparticles. J. Phys. Chem. B 105, 12689–12703.

Gerbig, C.A., Kim, C.S., Stegemeier, J.P., Ryan, J.N., Aiken, G.R., 2011. Formation of nanocolloidal metacinnabar in mercury-DOM-sulfide systems. Environ. Sci. Technol. 45, 9180–9187.

Gilmour, C.C., Elias, D.A., Kucken, A.M., Brown, S.D., Palumbo, A.V., Schadt, C.W., et al., 2011. Sulfate-reducing bacterium *Desulfovibrio desulfuricans* ND132 as a model for understanding

bacterial mercury methylation. Appl. Environ. Microbiol. 77, 3938.
Graham, A.M., Aiken, G.R., Gilmour, C.C., 2012. Dissolved organic matter enhances microbial mercury methylation under sulfidic conditions. Environ. Sci. Technol. 46, 2715–2723.
Haitzer, M., Aiken, G.R., Ryan, J.N., 2002. Binding of mercury(II) to dissolved organic matter: the role of the mercury-to-DOM concentration ratio. Environ. Sci. Technol. 36, 3564–3570.
Haskins, D.L., Gogal, R.M., Tuberville, T.D., 2020. Snakes as novel biomarkers of mercury contamination: a review. Rev. Environ. Contam. Toxicol. 249, 133–152.
He, X., McAlliser, D., Aker, W.G., Hwang, H., 2016. Assessing the effect of different natural dissolved organic matters on the cytotoxicity of titanium dioxide nanoparticles with bacteria. J. Environ. Sci. 48, 230–236.
Hesterberg, D., Chou, J.W., Hutchison, K.J., Sayers, D.E., 2001. Bonding of Hg(II) to reduced organic sulfur in humic acid as affected by S/Hg ratio. Environ. Sci. Technol. 35, 2741–2745.
Higueras, P., Oyarzun, R., Biester, H., Lillo, J., Lorenzo, S., 2003. A first insight into mercury distribution and speciation in soils from the Almaden mining district, Spain. J. Geochem. Explor. 80 (1), 95–104.
Hochella Michael, F., Lower Steven, K., Maurice Patricia, A., Penn, R.L., Sahai, N., Sparks Donald, L., et al., 2008. Nanominerals, mineral nanoparticles, and earth systems. Science 319, 1631–1635.
Hsu-Kim, H., Kucharzyk, K.H., Zhang, T., Deshusses, M.A., 2013. Mechanisms regulating mercury bioavailability for methylating microorganisms in the aquatic environment: a critical review. Environ. Sci. Technol. 47, 2441–2456.
Janadri, S., Mishra, A.P., Kumar, R., Shanmukh, I., Rao, N., Kharya, M., 2015. Preparation and characterization of mercury-based traditional herbomineral formulation: *Shwas kuthar rasa*. J. Ayurveda Integr. Med. 6, 268–272.
Jeong, H.Y., Klaue, B., Blum, J.D., Hayes, K.F., 2007. Sorption of mercuric ion by synthetic nanocrystalline mackinawite (FeS). Environ. Sci. Technol. 41, 7699–7705.
Jeong, H.Y., Sun, K., Hayes, K.F., 2010. Microscopic and spectroscopic characterization of Hg(II) immobilization by mackinawite (FeS). Environ. Sci. Technol. 44, 7476–7483.
Ji, X., Yang, L., Wu, F., Yao, L., Yu, B., Liu, X., et al., 2022. Identification of mercury-containing nanoparticles in the liver and muscle of cetaceans. J. Hazard. Mater. 424, 127759.
Ji, Y., Yang, Q., Zhang, T., 2020. Formation and structure of mercury-sulfide-iron nanoparticles and their role in the microbial production of methylmercury in soil and sediment pore water. Environ. Chem. 39, 1–7 (in Chinese).
Jiang, P., Li, Y.B., Liu, G.L., Yang, G.D., Lagos, L., Yin, Y.G., et al., 2016. Evaluating the role of re-adsorption of dissolved Hg^{2+} during cinnabar dissolution using isotope tracer technique. J. Hazard. Mater. 317, 466–475.
Jiang, T., Kaal, J., Liu, J., Liang, J., Zhang, Y., Wang, D., 2020. Linking the electron donation capacity to the molecular composition of soil dissolved organic matter from the Three Gorges Reservoir areas, China. J. Environ. Sci. 90, 146–156.
Jonsson, S., Skyllberg, U., Nilsson, M.B., Westlund, P.O., Shchukarev, A., Lundberg, E., et al., 2012. Mercury methylation rates for geochemically relevant Hg-II species in sediments. Environ. Sci. Technol. 46, 11653–11659.
Jun, Y.W., Casula, M.F., Sim, J.H., Kim, S.Y., Cheon, J., Alivisatos, A.P., 2003. Surfactant-assisted elimination of a high energy facet as a means of controlling the shapes of TiO_2 nanocrystals. J. Am. Chem. Soc. 125, 15981–15985.
Kellerman, A.M., Guillemette, F., Podgorski, D.C., Aiken, G.R., Butler, K.D., Spencer, R.G.M., 2018. Unifying concepts linking dissolved organic matter composition to persistence in aquatic ecosystems. Environ. Sci. Technol. 52, 2538–2548.
Kelly, D.J.A., Budd, K., Lefebvre, D.D., 2007. Biotransformation of mercury in pH-stat cultures of eukaryotic freshwater algae. Arch. Microbiol. 187, 45–53.
Kocman, D., Vreča, P., Fajon, V., Horvat, M., 2011. Atmospheric distribution and deposition of mercury in the Idrija Hg mine region. Slovenia. Environ. Res. 111, 1–9.
Lei, C., Sun, Y., Tsang, D.C.W., Lin, D., 2018. Environmental transformations and ecological effects of iron-based nanoparticles. Environ. Pollut. 232, 10–30.
Lei, P., Tang, C., Wang, Y., Wu, M., Kwong, R.W.M., Jiang, T., et al., 2021a. Understanding the effects of sulfur input on mercury methylation in rice paddy soils. Sci. Total Environ. 778, 146325.
Lei, P., Zhang, J., Zhu, J., Tan, Q., Kwong, R.W.M., Pan, K., et al., 2021b. Algal organic matter drives methanogen-mediated methylmercury production in water from eutrophic shallow lakes. Environ. Sci. Technol. 55, 10811–10820.
Li, C., Shen, J., Zhang, J., Lei, P., Kong, Y., Zhang, J., et al., 2021. The silver linings of mercury: reconsideration of its impacts on living organisms from a multi-timescale perspective. Environ. Int. 155, 106670.
Li, C., Yang, H., Du, Y., Xiao, Y., Zhandui, S., Zhang, W., et al., 2016a. Chemical species, micromorphology, and XRD fingerprint analysis of Tibetan medicine *Zuotai* containing mercury. Bioinorg. Chem. Appl. 2016, 7010519.
Li, P., Su, M., Wang, X., Zou, X., Sun, X., Shi, J., et al., 2020. Environmental fate and behavior of silver nanoparticles in natural estuarine systems. J. Environ. Sci. 88, 248–259.
Li, T., Senesi, A.J., Lee, B., 2016b. Small angle X-ray scattering for nanoparticle research. Chem. Rev. 116 (18), 11128–11180.
Li, Y., Gong, X., 2021. Effects of dissolved organic matter on the bioavailability of heavy metals during microbial dissimilatory iron reduction: a review. Rev. Environ. Contam. Toxicol. 257, 69–92.
Liang, D., Wang, X., Wang, Y., Dong, Z., Zhao, X., Fan, W., 2020. The dual effect of natural organic matter on the two-step internalization process of Au@SiO_2 in freshwater. Water Res 184, 116216.
Lino, A.S., Kasper, D., Guida, Y.S., Thomaz, J.R., Malm, O., 2019. Total and methyl mercury distribution in water, sediment, plankton and fish along the Tapajós River basin in the Brazilian Amazon. Chemosphere 235, 690–700.
Liu, J., Valsaraj, K.T., Devai, I., DeLaune, R.D., 2008. Immobilization of aqueous Hg(II) by mackinawite (FeS). J. Hazard. Mater. 157, 432–440.
Liu, J., Zhang, F., Ravikanth, V., Olajide, O.A., Li, C., Wei, L.X., 2019. Chemical compositions of metals in *Bhasmas* and Tibetan *Zuotai* are a major determinant of their therapeutic effects and toxicity. Evid. Based Complement Altern. Med., 1697804.
Liu, X., Liu, R., Chen, G.W., Luo, X.E., Lu, M.Q., 2020. Natural HgS nanoparticles in sulfide minerals from the Hetai goldfield. Environ. Chem. Lett. 18, 941–947.
Loosli, F., Le Coustumer, P., Stoll, S., 2013. TiO_2 nanoparticles aggregation and disaggregation in presence of alginate and Suwannee river humic acids. pH and concentration effects on nanoparticle stability. Water Res. 47, 6052–6063.
Louie, S.M., Tilton, R.D., Lowry, G.V., 2013. Effects of molecular weight distribution and chemical properties of natural organic matter on gold nanoparticle aggregation. Environ. Sci. Technol. 47 (9), 4245–4254.
Lowry, G.V., Shaw, S., Kim, C.S., Rytuba, J.J., Brown, G.E., 2004. Macroscopic and microscopic observations of particle-facilitated mercury transport from New Idria and sulphur bank mercury mine tailings. Environ. Sci. Technol. 38, 5101–5111.
Lu, D., Luo, Q., Chen, R., Zhuansun, Y., Jiang, J., Wang, W., et al., 2020. Chemical multi-fingerprinting of exogenous ultrafine particles in human serum and pleural effusion. Nat. Commun. 11, 2567.

Luo, H.W., Yin, X., Jubb, A.M., Chen, H., Lu, X., Zhang, W., et al., 2017. Photochemical reactions between mercury (Hg) and dissolved organic matter decrease Hg bioavailability and methylation. Environ. Pollut. 220, 1359–1365.
Ly, Q.V., Maqbool, T., Zhang, Z., Van Le, Q., An, X., Hu, Y., et al., 2021. Characterization of dissolved organic matter for understanding the adsorption on nanomaterials in aquatic environment: a review. Chemosphere 269, 128690.
Manceau, A., Enescu, M., Simionovici, A., Lanson, M., Gonzalez-Rey, M., Rovezzi, M., et al., 2016. Chemical forms of mercury in human hair reveal sources of exposure. Environ. Sci. Technol. 50 (19), 10721–10729.
Manceau, A., Lemouchi, C., Enescu, M., Gaillot, A.-C., Lanson, M., Magnin, V., et al., 2015. Formation of mercury sulfide from Hg(II)–thiolate complexes in natural organic matter. Environ. Sci. Technol. 49, 9787–9796.
Manceau, A., Wang, J., Rovezzi, M., Glatzel, P., Feng, X., 2018. Biogenesis of mercury–sulfur nanoparticles in plant leaves from atmospheric gaseous mercury. Environ. Sci. Technol. 52, 3935–3948.
Maurer-Jones, M.A., Gunsolus, I.L., Murphy, C.J., Haynes, C.L., 2013. Toxicity of engineered nanoparticles in the environment. Anal. Chem. 85, 3036–3049.
Mazrui, N.M., Jonsson, S., Thota, S., Zhao, J., Mason, R.P., 2016. Enhanced availability of mercury bound to dissolved organic matter for methylation in marine sediments. Geochim. Cosmochim. Acta 194, 153–162.
Mazrui, N.M., Seelen, E., King'ondu, C.K., Thota, S., Awino, J., Rouge, J., et al., 2018. The precipitation, growth and stability of mercury sulfide nanoparticles formed in the presence of marine dissolved organic matter. Environ. Sci. Proc. Imp. 20, 642–656.
Misra, S.K., Dybowska, A., Berhanu, D., Luoma, S.N., Valsami-Jones, E., 2012. The complexity of nanoparticle dissolution and its importance in nanotoxicological studies. Sci. Total Environ. 438, 225–232.
Mohd Omar, F., Abdul Aziz, H., Stoll, S., 2014. Aggregation and disaggregation of ZnO nanoparticles: influence of pH and adsorption of Suwannee river humic acid. Sci. Total Environ. 468-469, 195–201.
Morse, J.W., Luther, G.W., 1999. Chemical influences on trace metal-sulfide interactions in anoxic sediments. Geochim. Cosmochim. Acta 63, 3373–3378.
Mozhayeva, D., Engelhard, C., 2020. A critical review of single particle inductively coupled plasma mass spectrometry – a step towards an ideal method for nanomaterial characterization. J. Anal. Atom. Spectrom. 35, 1740–1783.
Mukhi, P., Mohapatra, S.S., Bhattacharjee, M., Ray, K.K., Muraleedharan, T.S., Arun, A., et al., 2017. Mercury based drug in ancient India: the red sulfide of mercury in nanoscale. J. Ayurveda Integr. Med. 8, 93–98.
Murphy, R., Strongin, D.R., 2009. Surface reactivity of pyrite and related sulfides. Surf. Sci. Rep. 64, 1–45.
Oyetibo, G.O., Miyauchi, K., Suzuki, H., Endo, G., 2016. Mercury removal during growth of mercury tolerant and self-aggregating *Yarrowia spp*. AMB Express 6, 99.
Oyetibo, G.O., Miyauchi, K., Suzuki, H., Endo, G., 2019. Bio-oxidation of elemental mercury during growth of mercury resistant yeasts in simulated hydrosphere. J. Hazard. Mater. 373, 243–249.
Parks, J.M., Johs, A., Podar, M., Bridou, R., Hurt, R.A., Smith, S.D., et al., 2013. The genetic basis for bacterial mercury methylation. Science 339, 1332–1335.
Patty, C., Barnett, B., Mooney, B., Kahn, A., Levy, S., Liu, Y., et al., 2009. Using X-ray microscopy and Hg L3 XANES to study Hg binding in the rhizosphere of *Spartina* cordgrass. Environ. Sci. Technol. 43, 7397–7402.
Pham, A.L.T., Morris, A., Zhang, T., Ticknor, J., Levard, C., Hsu-Kim, H., 2014. Precipitation of nanoscale mercuric sulfides in the presence of natural organic matter: Structural properties, aggregation, and biotransformation. Geochim. Cosmochim. Acta 133, 204–215.
Philippe, A., Schaumann, G.E., 2014. Interactions of dissolved organic matter with natural and engineered inorganic colloids: a review. Environ. Sci. Technol. 48, 8946–8962.
Poda, A.R., Kennedy, A.J., Cuddy, M.F., Bednar, A.J., 2013. Investigations of UV photolysis of PVP-capped silver nanoparticles in the presence and absence of dissolved organic carbon. J. Nanopart. Res. 15, 1673.
Poulin, B.A., Gerbig, C.A., Kim, C.S., Stegemeier, J.P., Ryan, J.N., Aiken, G.R., 2017. Effects of sulfide concentration and dissolved organic matter characteristics on the structure of nanocolloidal metacinnabar. Environ. Sci. Technol. 51, 13133–13142.
Proux, O., Lahera, E., Del Net, W., Kieffer, I., Rovezzi, M., Testemale, D., et al., 2017. High-energy resolution fluorescence detected X-ray absorption spectroscopy: a powerful new structural tool in environmental biogeochemistry sciences. J. Environ. Qual. 46 (6), 1146–1157.
Ravichandran, M., Aiken, G.R., Ryan, J.N., Reddy, M.M., 1999. Inhibition of precipitation and aggregation of metacinnabar (mercuric sulfide) by dissolved organic matter isolated from the Florida everglades. Environ. Sci. Technol. 33, 1418–1423.
Regnell, O., Watras, C.J., 2019. Microbial mercury methylation in aquatic environments: a critical review of published field and laboratory studies. Environ. Sci. Technol. 53, 4–19.
Rodrigues, P.D., Ferrari, R.G., dos Santos, L.N., Conte Junior, C.A., 2019. Mercury in aquatic fauna contamination: a systematic review on its dynamics and potential health risks. J. Environ. Sci. 84, 205–218.
Roth, V.N., Lange, M., Simon, C., Hertkorn, N., Bucher, S., Goodall, T., et al., 2019. Persistence of dissolved organic matter explained by molecular changes during its passage through soil. Nat. Geosci. 12, 755–761.
Ruhland, D., Nwoko, K., Perez, M., Feldmann, J., Krupp, E.M., 2019. AF4-UV-MALS-ICP-MS/MS, sp ICP-MS, and STEM-EDX for the characterization of metal-containing nanoparticles in gas condensates from petroleum hydrocarbon samples. Anal. Chem. 91, 1164–1170.
Satake, K., Shibata, K., Bando, Y., 1990. Mercury sulphide (HgS) crystals in the cell walls of the aquatic bryophytes, *Jungermannia vulcanicola* Steph. and *Scapania undulata* (L.) Dum. Aquat. Bot. 36, 325–341.
Sathyavathi, S., Manjula, A., Rajendhran, J., Gunasekaran, P., 2013. Biosynthesis and characterization of mercury sulphide nanoparticles produced by *Bacillus cereus* MRS-1. Indian J. Exp. Biol. 51, 973–978.
Scofield, M.E., Koenigsmann, C., Wang, L., Liu, H.Q., Wong, S.S., 2015. Tailoring the composition of ultrathin, ternary alloy PtRuFe nanowires for the methanol oxidation reaction and formic acid oxidation reaction. Energ. Environ. Sci. 8 (1), 350–363.
Selvaraj, R., Qi, K., Al-Kindy, S.M.Z., Sillanpaa, M., Kim, Y., Tai, C.W., 2014. A simple hydrothermal route for the preparation of HgS nanoparticles and their photocatalytic activities. RSC Adv. 4 (30), 15371–15376.
Si, L., Ariya, P.A., 2015. Photochemical reactions of divalent mercury with thioglycolic acid: formation of mercuric sulfide particles. Chemosphere 119, 467–472.
Singh, S., Chaudhary, A., Rai, D., Rai, S., Chaudhari, A., 2009. Preparation and characterization of a mercury based Indian traditional drug – *Rasa Sindoor*. J. Ayurveda Integr. Med. 31, 346–351.

Skyllberg, U., Drott, A., 2010. Competition between disordered iron sulfide and natural organic matter associated thiols for mercury(II)—an EXAFS study. Environ. Sci. Technol. 44, 1254–1259.
Slowey, A.J., 2010. Rate of formation and dissolution of mercury sulfide nanoparticles: the dual role of natural organic matter. Geochim. Cosmochim. Acta 74, 4693–4708.
Smith, R.S., Wiederhold, J.G., Kretzschmar, R., 2015. Mercury isotope fractionation during precipitation of metacinnabar (β-HgS) and montroydite (HgO). Environ. Sci. Technol. 49, 4325–4334.
Sunderland, E.M., Selin, N.E., 2013. Future trends in environmental mercury concentrations: implications for prevention strategies. Environ. Health 12 (2).
Tian, L., Guan, W., Ji, Y., He, X., Chen, W., Alvarez, P.J.J., Zhang, T., 2021a. Microbial methylation potential of mercury sulfide particles dictated by surface structure. Nat. Geosci. 14, 409–416.
Tian, L., Guan, W., Zhao, Z., Ji, Y., Zhang, T., 2021b. Influence of crystalline phase and exposed facet of nanocrystals on their environmental behavior and impacts. Environ. Chem. 40, 999–1010 (in Chinese).
Vogel, C., Krüger, O., Herzel, H., Amidani, L., Adam, C., 2016. Chemical state of mercury and selenium in sewage sludge ash based P-fertilizers. J. Hazard. Mater. 313, 179–184.
Wang, Z., Zhang, L., Zhao, J., Xing, B., 2016. Environmental processes and toxicity of metallic nanoparticles in aquatic systems as affected by natural organic matter. Environ. Sci. Nano. 3, 240–255.
Waples, J.S., Nagy, K.L., Aiken, G.R., Ryan, J.N., 2005. Dissolution of cinnabar (HgS) in the presence of natural organic matter. Geochim. Cosmochim. Acta 69 (6), 1575–1588.
Wolfenden, S., Charnock, J.M., Hilton, J., Livens, F.R., Vaughan, D.J., 2005. Sulfide species as a sink for mercury in lake sediments. Environ. Sci. Technol. 39, 6644–6648.
Wu, Y., Wang, W.X., 2014. Intracellular speciation and transformation of inorganic mercury in marine phytoplankton. Aquat. Toxicol. 148, 122–129.
Xu, J., Bland, G.D., Gu, Y., Ziaei, H., Xiao, X., Deonarine, A., et al., 2021. Impacts of sediment particle grain size and mercury speciation on mercury bioavailability potential. Environ. Sci. Technol. 55 (18), 12393–12402.
Yan, L.F., 2007. Analysis of microstructure and composition of Tibetan medicine "*Zuotai*". J. Chin. Med. Mater. 36, 583–585 (in Chinese).
Yan, S., Liu, Y., Lian, L., Li, R., Ma, J., Zhou, H., Song, W., 2019. Photochemical formation of carbonate radical and its reaction with dissolved organic matters. Water Res. 161, 288–296.
Yan, Y., Du, J.S., Gilroy, K.D., Yang, D., Xia, Y., Zhang, H., 2017. Intermetallic nanocrystals: syntheses and catalytic applications. Adv. Mater. 29, 1605997.
Yu, S., Liu, J., Yin, Y., Shen, M., 2018. Interactions between engineered nanoparticles and dissolved organic matter: a review on mechanisms and environmental effects. J. Environ. Sci. 63, 198–217.
Zark, M., Dittmar, T., 2018. Universal molecular structures in natural dissolved organic matter. Nat. Commun. 9, 3178.
Zhang, T., Kim, B., Levard, C., Reinsch, B.C., Lowry, G.V., Deshusses, M.A., et al., 2012. Methylation of mercury by bacteria exposed to dissolved, nanoparticulate, and microparticulate mercuric sulfides. Environ. Sci. Technol. 46, 6950–6958.
Zhang, T., Kucharzyk, K.H., Kim, B., Deshusses, M.A., Hsu-Kim, H., 2014. Net methylation of mercury in estuarine sediment microcosms amended with dissolved, nanoparticulate, and microparticulate mercuric sulfides. Environ. Sci. Technol. 48, 9133–9141.
Zhang, Z., Si, R., Lv, J., Ji, Y., Chen, W., Guan, W., et al., 2020. Effects of extracellular polymeric substances on the formation and methylation of mercury sulfide nanoparticles. Environ. Sci. Technol. 54, 8061–8071.